Mechanism for singular behavior in vibrational spectra of topologically disordered systems: Short-range attractions

Ten-Ming Wu, S. L. Chang, and K. H. Tsai

Citation: The Journal of Chemical Physics **122**, 204501 (2005); doi: 10.1063/1.1900726
View online: http://dx.doi.org/10.1063/1.1900726
View Table of Contents: http://scitation.aip.org/content/aip/journal/jcp/122/20?ver=pdfcov
Published by the AIP Publishing

Mechanism for singular behavior in vibrational spectra of topologically disordered systems: Short-range attractions

Ten-Ming Wu,[a] S. L. Chang,[b] and K. H. Tsai
Institute of Physics, National Chiao-Tung University, Hsin chu, Taiwan, Republic of China

(Received 19 November 2004; accepted 10 March 2005; published online 20 May 2005)

At low-enough fluid densities, we have found some naive singular behavior, like the van Hove singularities in the phonon spectra of lattices, appearing in the instantaneous normal mode spectra of the Lennard-Jones (LJ) 2*n*-*n* fluids, which serve as a prototype of topologically disordered systems. The singular behavior cannot be predicted by the mean-field theory, but interpreted by the perturbed binary modes of some special pairs, called the mutual nearest neighbor pairs, at separations corresponding to the extreme binary frequencies, which are solely determined by the attractive part of the LJ 2*n*-*n* pair potential. By reducing the range of attraction in the pair potential under the conditions of the same particle diameter and well depth, the tendency for the appearance of the singular behavior shifts to higher fluid densities. From this study, we conclude that pair potential with a short-range attraction can be a mechanism to produce a counterpart of the van Hove singularity in the vibrational spectra of disordered systems without a reference lattice. © *2005 American Institute of Physics*. [DOI: 10.1063/1.1900726]

I. INTRODUCTION

Recently, vibrational spectra of disordered systems have received many theoretical studies. In either scalar or vector atomic motions, several proposed lattice models of disordered force constants,[1–4] which are treated as random variables subject to a certain probability distribution, have produced the boson peak,[5] the low-frequency excess vibrational density of states (DOS) compared to the Debye law, in numerical calculations and the coherent potential approximation. The produced boson peak is found to reduce to the lowest van Hove singularity of the reference lattice as disorder is vanished. Also, its position is pushed to low frequencies by softening the force constants even with the presence of negative values; this is consistent with the shifting of the boson peak observed in some glasses by increasing temperature.[6] These models are critically based on a reference lattice. It is well known that the van Hove singularities of a lattice are smeared out as the atomic positions become random.[7] Then, it raises a fundamental question: Can a counterpart of the van Hove singularity exist in the systems with atomic positions as disordered as in glasses and liquid states, which are termed as topologically disordered systems, if so, what is the mechanism to produce it?

It is helpful in the present days to give a brief summary on the van Hove singularities of lattices, before considering the topologically disordered systems. Pointed out by van Hove in five decades ago,[8] for a lattice under the harmonic approximation, it is the periodicity of the lattice that necessarily implies the existence of critical points, where the gradients of the phonon frequency vanish, on the surfaces of constant frequency in the reciprocal space. According to the surface curvatures at a point, the critical points can be classified into three different kinds: a local maximum, a local minimum, and a saddle. The vanishing gradient at a critical point gives rise to a singularity in the phonon DOS, which is proportional to an integral over the constant-frequency surface inversely weighted by the magnitude of the gradient of the phonon frequency in the reciprocal space. Hence, the locations of the singularities in a phonon spectrum are determined by the frequencies of these critical points, and the general behavior near a singularity is strictly subject to the curvature characteristic of the associated critical point and the spatial dimension of the lattice.

Simple fluids serve as a prototype of topologically disordered systems. The vibrational motions of particles in a simple fluid at an instant is described by the Hessian matrix of the corresponding configuration. Lacking periodicity in fluid structure, the Hessian matrices of a simple fluid are diagonalized in the real space rather than in the reciprocal space, and the eigenmodes of each matrix are referred as the instantaneous normal modes (INMs) of the fluid. The INM frequency spectrum is a distribution of the square roots of the eigenvalues averaged over configurations.[9,10] Due to the vector nature of particle displacements, the Hessian matrices are composed of diagonal and off-diagonal blocks of spatial dimension, with their elements obeying the sum rules due to momentum conservation, which makes sure for each Hessian matrix the existence of zero-value eigenvalues.[11,12] For particles interacting via a pair potential $\phi(r)$ in three-dimensional space, the negative of each off-diagonal block $\mathbf{t}(\mathbf{r})$, which is associated with a pair of two particles at a relative position $\mathbf{r}$, can be separated into the longitudinal part $\mathbf{t}_L(\mathbf{r})=\phi''(r)\hat{\mathbf{r}}\hat{\mathbf{r}}$ and the transverse part $\mathbf{t}_T(\mathbf{r})=\phi'(r)/r(\mathbf{I}_3-\hat{\mathbf{r}}\hat{\mathbf{r}})$, corresponding to the vibrational and rotational motions of the two particles at the instant, respectively. Here, $\hat{\mathbf{r}}$ is the

[a]Author to whom correspondence should be addressed. Electronic mail: tmw@faculty.nctu.edu.tw
[b]Present address: Department of Computer Science and Information Engineering, National Peng-Hu Institute of Technology, Peng-Hu, Taiwan.

unit vector along $\mathbf{r}$ and $\mathbf{I}_3$ is the unit matrix in three dimensions. Therefore, the Hessian matrices are an ensemble of the so-called Euclidean random matrices whose elements are given by some deterministic functions of the distances between particles, with randomness originating from the disorder of particle positions among configurations.[13] Recently, a perturbative approach, called Euclidean random matrix theory, is developed for calculating the dynamic structure factors and vibrational spectra of topologically disordered systems.[14–16] For the INM spectra of simple fluids reported so far, a singularity at zero value in the eigenvalue spectrum, caused by the sum rules due to momentum conservation, has been reported for a liquid model.[17] Nevertheless, a high-frequency peak in the INM spectrum, analogous to the van Hove singularity, is predicted by Euclidean random matrix theory for a Gaussian model.[16]

For most of realistic simple fluids, the pair potential $\phi(r)$ between two particles is composed of the repulsive and attractive parts. Generally, the range of the repulsive part is determined by the size of a particle; however, the attractive part decays in magnitude with increasing distance. For the usually studied Lennard-Jones (LJ) potential, the potential in the attractive part decays monotonically and has a reflection point, where $\phi''(r)=0$. The second derivative of the LJ potential, which we refer as the vibrational curvature of the pair potential, has a minimum at distance r_{vib}, and $\phi'(r)/r$, referred as the rotational curvature, has a maximum at r_{rot}, with r_{vib} larger than r_{rot}. For a pair potential with characteristics similar as the LJ potential, but shortened in the attractive range by a fast decay in the tail, both r_{vib} and r_{rot} decrease in value as compared with the particle size; also, the absolute values of the minimum vibrational curvature and the maximum rotational curvature increase. For the INM spectrum of such a simple fluid, the two curvature extrema, with one giving the lower limit on the magnitude of $\mathbf{t}_L(\mathbf{r})$ and the other giving the upper limit on the magnitude of $\mathbf{t}_T(\mathbf{r})$ in the Hessian matrices, may be considered as the counterpart of the critical points in the reciprocal space of a lattice, with the following argument.

It has been evidenced numerically that in the simple LJ fluids at high densities the characters of the INMs in the high-frequency end of the real branch are dominated by the so-called mutual nearest-neighbor (MNN) pairs, which are the two particles as nearest neighbors of each other in the fluid.[18] In the fluids at high densities, due to the highly compact local structures, the pair separations of the MNN pairs are so short that all forces between the two particles of these pairs are repulsive. As the fluid density decreases, the mean nearest-neighbor separation of the fluid generally increases. Once the fluid density is low enough, it is possible to find a significant amount of the MNN pairs with their separations exceeding r_{rot}, or even r_{vib}, with the forces between the two particles of these pairs being attractive. In such a situation, a pileup of the INMs dominated by the MNN pairs with separations near r_{rot} or r_{vib} is expected to produce a singularity, surviving a perturbation from the rest particles in the fluid, in the INM spectrum. Thus, the positions of the singularities in the INM frequency spectrum are simply related to the square roots of the extreme curvatures of the pair potential.

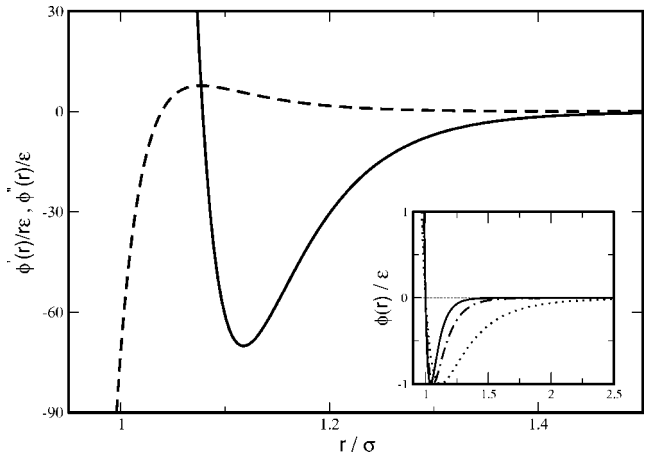

FIG. 1. Vibrational curvature $\phi''(r)$ (solid line) and rotational curvature $\phi'(r)/r$ (dashed line) of the LJ $2n$-n potential $\phi(r)$ for $n=18$. The inset shows the LJ $2n$-n potentials of $n=6$ (dotted line), 12 (dot-dashed line), and 18 (solid line) with the same particle diameter σ and well depth ϵ.

In this paper, we present the appearance of singular behavior in the INM spectra of simple fluids with short-range attractions, a model system for the colloid-polymer mixtures, which have recently received considerable attention.[19] In Sec. II, we give the pair potential of our model and the INM spectra of the considered fluids. The density and temperature variations of the singularity in the INM spectrum are also examined. Given in Sec. III is the exposition for the physical origin of the INM singularities. In Sec. IV, we give our conclusions.

II. PAIR POTENTIAL AND THE INM SPECTRA

We consider systems of atomic particles with mass m interacting via the pairwise additive LJ $2n-n$ potential

$$\phi(r)=4\epsilon\left[\left(\frac{\sigma}{r}\right)^{2n}-\left(\frac{\sigma}{r}\right)^{n}\right], \tag{1}$$

where ϵ is the well depth of the potential, and the particle diameter σ is the distance at which $\phi(r)=0$. n is a parameter for tuning the range of the potential with fixed ϵ and σ. The minimum and the reflection point of the potential are, respectively, at $r_{\mathrm{min}}=2^{1/n}\sigma$ and $r_{\mathrm{ref}}=[2(2n+1)/(n+1)]^{1/n}\sigma$, which are both larger than σ. As n increases, both r_{min} and r_{ref} move toward σ, indicating that the interaction range of the LJ $2n$-n potential becomes shorter with increasing n under the conditions of the same well depth and particle diameter. The potential with $n=6$, which has been extensively studied, has a long interaction range. The potential with $n=12$, which is very similar to the one describing the C_{60} system,[20] has a medium range. For $n=18$, the potential becomes short range and is close to the hard-sphere attractive Yukawa potential,[21] which is used to describe the interactions between colloids mixed in a nonabsorbing polymer. The LJ $2n$-n potentials of these three n values are shown in the inset of Fig. 1. The vibrational and rotational curvatures of $\phi(r)$ are shown in Fig. 1 for $n=18$. Due to the attractive part of $\phi(r)$, the rotational curvature has a maximum at r_{rot} and the vibrational curvature has a minimum at r_{vib}, where

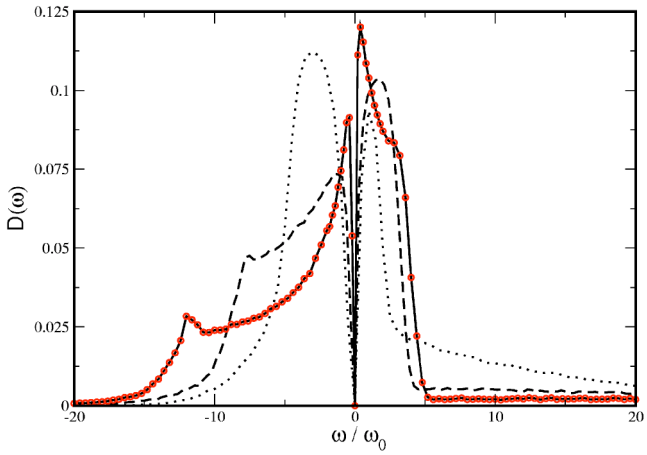

FIG. 2. INM DOS of the LJ $2n$-n fluids at $\rho^*=0.3$ and $T^*=1.4$. The dotted, dashed, and solid lines are for $n=6$, 12, and 18, respectively. The open circles stand for the simulation data. As is standard, the imaginary-frequency spectrum is displayed along the negative frequency axis. Frequencies in the abscissa are in units of the characteristic LJ frequency $\omega_0=(\epsilon/m\sigma^2)^{1/2}$.

$$r_{\mathrm{rot}}=\left(\frac{4(n+1)}{n+2}\right)^{1/n}\sigma, \tag{2}$$

$$r_{\mathrm{vib}}=\left(\frac{4(2n+1)}{n+2}\right)^{1/n}\sigma. \tag{3}$$

Using the periodic boundary conditions and the minimum image convention for 864 particles in a cubic box, we have performed molecular-dynamics simulations in the isothermal-isochoric ensemble for the LJ $2n$-n fluids with $n=6$, 12, and 18.[22] For each simulation, we set the time step $\Delta t^*=0.001$ in reduced unit. The reduced units used in this paper are $T^*=k_BT/\epsilon$ for temperature, $\rho^*=\rho\sigma^3$ for density, and $t^*=t/t_0$ for time, where $t_0=(m\sigma^2/\epsilon)^{1/2}$. After one hundred fluid configurations were generated, their Hessian matrices were calculated and diagonalized, and the DOS of the INMs were obtained.

At the same reduced density ($\rho^*=0.3$) and reduced temperature ($T^*=1.4$), the calculated INM DOS for three different ranges of the pair potential ($n=6$, 12, and 18) are shown in Fig. 2. The chosen reduced temperature is above the critical temperatures of the three LJ $2n$-n fluids.[23] The INM DOS of $n=6$ behaves smoothly for both branches. However, as the interaction range of the pair potential becomes shorter, some naive behavior shows up, first in the imaginary branch and then in the real. For $n=12$, a shoulder appears in the middle region of the imaginary branch and a small cusp near $7.6\omega_0$ ($\omega_0=t_0^{-1}$) can be clearly observed on the corner of the shoulder. As the interaction range is shortened to the case of $n=18$, the spectra of the real and imaginary branches are further changed. Near zero frequency, both branches have a very steep linear spectrum, which is due to the factor arising from transferring the eigenvalue spectrum to the frequency one.[10,11] In addition, the spectrum has a shoulder near $3.2\omega_0$ in the real branch, and a very sharp cusp at $11.84\omega_0$ in the imaginary branch. As far as we know, a cusp appearing in the INM spectrum has not been reported for any simple fluids.

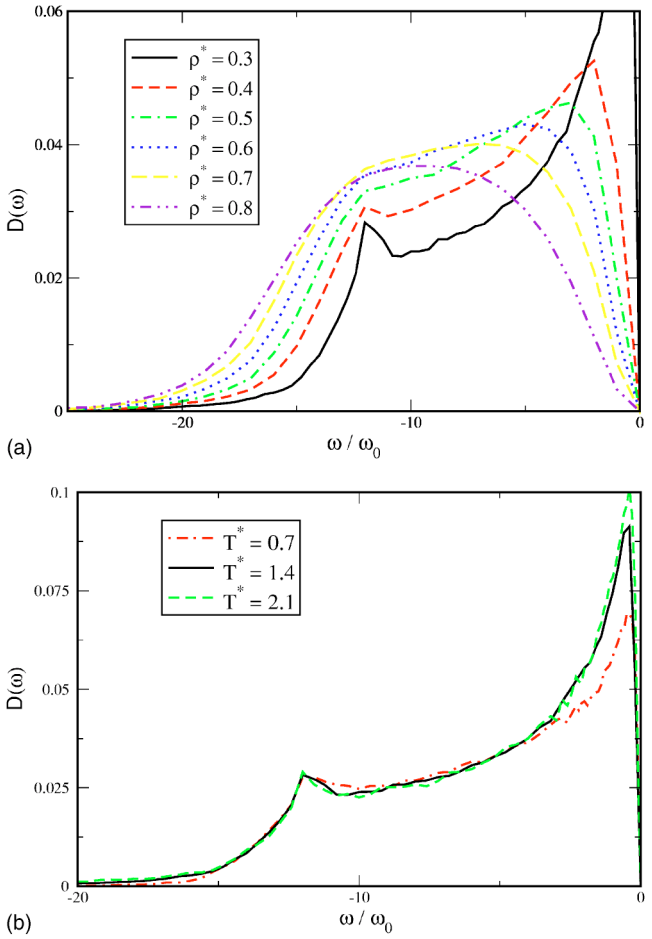

FIG. 3. Density (a) and temperature (b) variations of the imaginary INM DOS of the LJ $2n$-n fluids for $n=18$ at $T^*=1.4$ in (a) and at $\rho^*=0.3$ in (b).

Thus, to investigate the physical origin of the cusp in the INM spectrum of a LJ $2n$-n fluid is the main theme of this paper.

We first examine how sensitively the cusp changes with thermodynamic variables. Shown in Fig. 3 are the variations of the imaginary-INM spectrum with density and temperature for the LJ $2n$-n fluid of $n=18$. Generally, the cusp is smeared out by increasing the fluid density: By increasing density from $\rho^*=0.3$ but keeping temperature fixed, the cusp shrinks first at $\rho^*=0.4$, then changes to be a shoulder at $\rho^*=0.6$, and completely disappears at $\rho^*=0.8$; the whole imaginary spectrum recovers back to be smooth at high densities. On the other hand, by fixing the reduced density at 0.3, the change of the cusp with temperature is not so sensitive, as T^*, still above the critical temperature, increases from 0.7 to 2.1. As the temperature is varied, the cusp is still clearly identified, without noticeable changes in its position and the value of the DOS at the cusp. Only the shape of the spectrum at the low-frequency side of the cusp is somewhat changed with temperature.

The INM spectrum of a simple fluid can be calculated by a mean-field (MF) theory,[11] which is in analogy to the coherent potential approximation for the lattice models of disordered force constants, with the required inputs: the fluid density, the vibrational and rotational curvatures of a pair potential and the radial distribution function $g(r)$. The MF

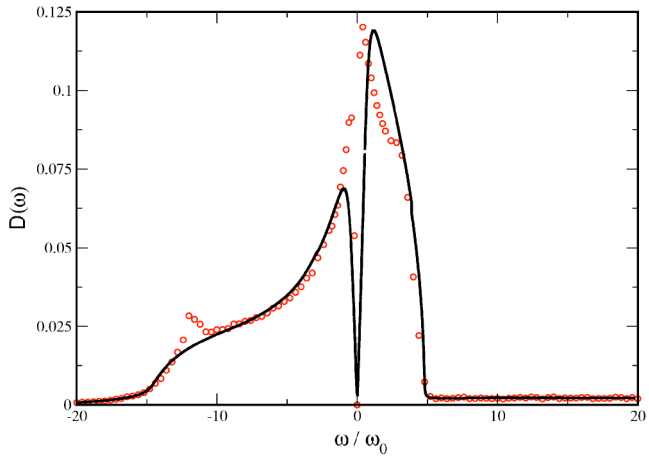

FIG. 4. Comparison of the INM DOS of the LJ $2n$-n fluid for $n=18$ at $\rho^*=0.3$ and $T^*=1.4$ calculated by the mean-field theory (solid line) with the simulation results (open circles).

theory has been tested for a LJ $2n$-n fluid of $n=6$ and good agreement with numerical simulations has been achieved. Also, the MF theory has been calculated for various simple fluids, including liquid Na and fluids with pure repulsive LJ potential;[24] however, as far as we know, simple fluids with short-range attractions have not been tested. Therefore, we calculated with the MF theory the INM DOS of the LJ $2n$-n fluid for $n=18$ at $\rho^*=0.3$ and $T^*=1.4$. Shown in Fig. 4 is the comparison of the calculated results with the simulation data. The whole INM spectrum of the fluid can be generally described by the MF theory, except for the cusp in the imaginary branch and the shoulder in the real.

III. MNN PAIRS AND THEIR PERTURBED BINARY MODES

In order to explain the physical origin of the cusp in the INM spectrum, we have studied the distribution of the MNN pairs in the LJ $2n$-n fluids.[18,25] The MNN pairs were first studied for solvation dynamics and vibrational population relaxation in liquids,[18] and later for vibrational and rotational energy relaxations in fluids.[26,27] The concept of the MNN pair was also used to interpret the infrared Q-branch absorption of HCl in liquid Ar.[28]

In an atomic fluid, the distribution, $g_{\mathrm{MNN}}(r)$, of the MNN paris as a function of pair separation r is defined in the following: For an arbitrary particle, $\rho g_{\mathrm{MNN}}(r)$ is the probability density to find a second particle at a distance r away from the first one with these two being a MNN pair. The $g_{\mathrm{MNN}}(r)$ distributions of two LJ fluids at $\rho^*=0.3$ and $T^*=1.4$ are presented in Fig. 5(a), with one for a pair potential of long range ($n=6$) and the other for short range ($n=18$). For the sake of comparison, the ordinary radial distribution functions of the two fluids are also shown in Fig. 5(a), and the distances r_{rot} and r_{vib} of each pair potential are indicated. At reduced desnity as low as 0.3, no matter how long the range of the pair potential is, the shape of the $g_{\mathrm{MNN}}(r)$ distribution is no longer a Gaussian as the cases at high densities.[25] Clearly, $g_{\mathrm{MNN}}(r)$ at small r is subject to $g(r)$, where the two distributions are determined by the repulsive core of the pair potential. On the other hand, the tail of the $g_{\mathrm{MNN}}(r)$ distribution is

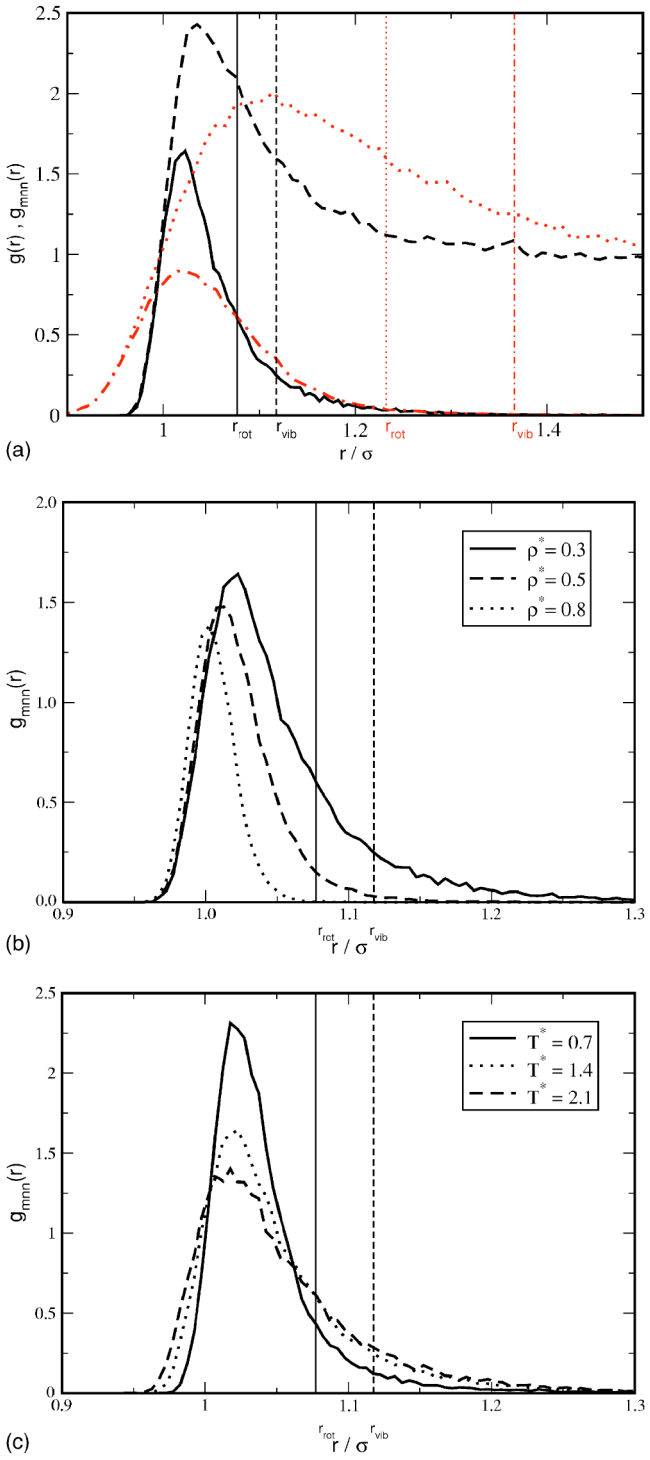

FIG. 5. (a) The distributions $g_{\mathrm{MNN}}(r)$ of mutual nearest neighbor pairs in the LJ $2n$-n fluids with $n=18$ (thick solid line) and $n=6$ (thick dot-dashed line) at $\rho^*=0.3$ and $T^*=1.4$. The radial distribution functions $g(r)$ of the two fluids are given by the thick dashed ($n=18$) and dotted ($n=6$) lines. The thinner solid and dashed straight lines indicate the r_{rob} and r_{vib} positions of the LJ $2n$-n potential for $n=18$, respectively; the thinner dotted and dot-dashed lines indicate those positions of the potential for $n=6$. (b) Density variation of $g_{\mathrm{MNN}}(r)$ for $n=18$ at $T^*=1.4$. (c) Temperature variation of $g_{\mathrm{MNN}}(r)$ for $n=18$ at $\rho^*=0.3$.

almost the same for the two fluids. However, the tail extends much over both the distances r_{rot} and r_{vib} for the case of $n=18$, but is almost vanished at r_{vib} for the case of $n=6$.

For $n=18$, the density and temperature variations of the

$g_{\mathrm{MNN}}(r)$ distribution are shown in Figs. 5(b) and 5(c), respectively. As density increases, the major impact on the distribution is the shrinkage of its tail, in addition to an inward shift in the position of its maximum. At reduced density equal to 0.8, the distribution is almost terminated at the r_{rot} distance of the LJ $2n$-n potential of $n=18$ due to a rather compact local structure, which gives a significantly decreasing in the distances between each particle and its neighbors. By reducing the fluid temperature but keeping fluid density the same, the $g_{\mathrm{MNN}}(r)$ distribution has a narrower width and an enhanced maximum at almost similar position, but still widely extends over r_{vib}. Therefore, the value of $g_{\mathrm{MNN}}(r)$ at r_{vib} is essentially dominated by the fluid density, but gently varies with temperature.

During the lifetime of a MNN pair in a fluid,[25] the relative motion of the two particles can be approximately described by the binary modes of the MNN pair under a perturbation from other particles in the fluid. In the zeroth order of the perturbation, the two particles of a MNN pair, with index i and j, are considered to be isolated from the rest particles. Interacting via the pair potential $\phi(r)$ at a separation r_{ij} in three-dimensional space, the two particles have one vibrational and two degenerate rotational binary modes[29] with their frequencies given by

$$\omega_{\mathrm{vib},0}(r_{ij}) = \sqrt{\frac{2\phi''(r_{ij})}{m}}, \tag{4}$$

$$\omega_{\mathrm{rot},0}(r_{ij}) = \sqrt{\frac{2\phi'(r_{ij})}{mr_{ij}}}, \tag{5}$$

where the 0 subscript indicates the isolation of the two particles. Because of the equality in their masses, the six-dimensional eigenvector of each binary mode consists of two three-dimensional vectors, equal in magnitude but different in sign, with each vector indicating the motion of one particle in this mode. For the vibrational binary mode, the three-dimensional vector is simply $\hat{\mathbf{r}}_{ij}/\sqrt{2}$, where $\sqrt{2}$ is due to the normalization of the six-dimensional eigenvector, and the two particles move along the line connecting them. The corresponding vectors of the two degenerate rotational binary modes are $\hat{\theta}_{\mathbf{1}}(i,j)/\sqrt{2}$ and $\hat{\theta}_{\mathbf{2}}(i,j)/\sqrt{2}$, where $\hat{\theta}_{\mathbf{1}}(i,j)$ and $\hat{\theta}_{\mathbf{2}}(i,j)$ are two unit vectors orthogonal to $\hat{\mathbf{r}}_{ij}$ and to each other.[30] Hence, in each rotational binary mode, the two particles make a circular motion in a plane, and move perpendicularly to the line connecting them.

For the rotational and vibrational curvatures of the LJ $2n$-n potential shown in Fig. 1, the frequency of the rotational binary mode has a maximum, $\omega^*_{\mathrm{rot},0}$, with the pair separation at r_{rot}, and that of the vibrational binary mode has a minimum, $|\omega^*_{\mathrm{vib},0}|$, with the pair separation at r_{vib}, where $\omega^*_{\mathrm{vib},0}$ is pure imaginary for $\phi''(r_{\mathrm{vib}})$ being negative and $|A|$ is the absolute value of a complex number A. The two extreme binary-mode frequencies are only determined by n, the parameter controlling the range of the pair potential, and can be explicitly expressed as

$$\frac{\omega^*_{\mathrm{rot},0}}{\omega_0} = \frac{n}{n+1}\sqrt{n+2}\left(\frac{n+2}{4(n+1)}\right)^{1/n}, \tag{6}$$

$$\frac{|\omega^*_{\mathrm{vib},0}|}{\omega_0} = n\sqrt{\frac{n+2}{2n+1}}\left(\frac{n+2}{4(2n+1)}\right)^{1/n}. \tag{7}$$

According to these expressions, as n is large enough, $\omega^*_{\mathrm{rot},0}$ is proportional to $\sqrt{n}$ and $|\omega^*_{\mathrm{vib},0}|$ to n. Also, evaluated for $n=18$, $\omega^*_{\mathrm{rot},0}$ and $|\omega^*_{\mathrm{vib},0}|$ are $3.93\omega_0$ and $11.84\omega_0$, which are almost the position of the shoulder and exactly that of the cusp in the INM spectrum shown in Fig. 2 for $n=18$, respectively. The reason why Eqs. (6) and (7) correctly predict the singularity positions in the INM spectrum is explained in the following.

The DOS of the binary modes of the isolated MNN pairs is defined as

$$D_{\eta,0}(\omega) = \left\langle \frac{1}{6N}{\sum_{i\neq j}}' \delta(\omega - \omega_{\eta,0}(r_{ij})) \right\rangle, \tag{8}$$

where η can be either rot or vib and the prime in the summation indicates that particles i and j are a MNN pair. The bracket stands for an ensemble average. The normalization factor is $6N$ rather than $3N$ for each MNN pair is counted twice in the formula. In terms of the MNN pair distribution, the DOS can be expressed as

$$D_{\eta,0}(\omega) = \frac{4\pi\rho}{6}\int_0^\infty \delta(\omega - \omega_{\eta,0}(r))r^2 g_{\mathrm{MNN}}(r)dr. \tag{9}$$

For a δ function with an argument of a function, we have the following identity:

$$\delta(\omega - \omega_{\eta,0}(r)) = \sum_{r_s}\frac{\delta(r-r_s)}{\left|\frac{d\omega_{\eta,0}(r)}{dr}\right|_{r=r_s}} \tag{10}$$

with r_s being a root of the equation,

$$f_\eta(r) = \frac{m\omega^2}{2}, \tag{11}$$

where $f_{\mathrm{vib}}(r)=\phi''(r)$ and $f_{\mathrm{rot}}(r)=\phi'(r)/r$ are the vibrational and rotational curvatures of the pair potential, respectively. After inserting this identity into Eq. (9), the formula for the binary-mode DOS of the isolated MNN pairs is given as

$$D_{\eta,0}(\omega) = m|\omega|\frac{2\pi\rho}{3}\sum_{r_s}\frac{r_s^2 g_{\mathrm{MNN}}(r_s)}{|f'_\eta(r_s)|}. \tag{12}$$

Some important information can be obtained from Eq. (12). We only analyze the DOS of the vibrational binary modes and the analysis can be generalized in a similar way for that of the rotational binary modes. Since the cusp in the INM spectrum is in the imaginary branch, we consider ω here to be imaginary and have an absolute value less than $|\omega^*_{\mathrm{vib},0}|$ $(0<|\omega|<|\omega^*_{\mathrm{vib},0}|)$. In such a case, Eq. (11) generally has two roots, with one larger than r_{vib} and the other smaller than r_{vib}. As $|\omega|$ approaches to $|\omega^*_{\mathrm{vib},0}|$, the two roots coalesce at r_{vib}. At $|\omega|=|\omega^*_{\mathrm{vib},0}|$, $f_{\mathrm{vib}}(r_{\mathrm{rib}})=-m|\omega^*_{\mathrm{vib},0}|^2/2$ is a minimum with $f'_{\mathrm{vib}}(r_{\mathrm{vib}})=0$, and $D_{\mathrm{vib},0}(\omega)$, therefore, diverges. However, the singularity is expected to appear only if the fluid has a significant value of $g_{\mathrm{MNN}}(r)$ at r_{vib}, and would get disappeared in case that the value of $g_{\mathrm{MNN}}(r)$ at r_{vib} diminishes and eventually vanishes as the fluid density increases. By making a harmonic approximation around the minimum, we have

$$f_{\rm vib}(r) \approx f_{\rm vib}(r_{\rm vib}) + \tfrac{1}{2} f''_{\rm vib}(r_{\rm vib})(r - r_{\rm vib})^2, \tag{13}$$

where $f''_{\rm vib}(r_{\rm vib}) = \phi''''(r_{\rm vib})$ is a positive number. After this approximation, the behavior of $D_{\rm vib,0}(\omega)$ near the singularity can be explicitly given as

$$D_{\rm vib,0}(\omega) = \begin{cases} \dfrac{C}{\sqrt{|\omega^*_{\rm vib,0}|^2 - |\omega|^2}} & \text{for } |\omega| < |\omega^*_{\rm vib,0}| \\ 0 & \text{for } |\omega| > |\omega^*_{\rm vib,0}|, \end{cases} \tag{14}$$

with

$$C = \frac{2\pi}{3} r^2_{\rm vib} \rho g_{\rm MNN}(r_{\rm vib}) \left(\frac{2|\phi''(r_{\rm vib})|}{\phi''''(r_{\rm vib})} \right)^{1/2}. \tag{15}$$

Physically, C is determined by two factors: the number of the MNN pairs with separation at $r_{\rm vib}$ and the dispersion factor of the vibrational curvature $f_{\rm vib}(r)$, which plays a role here similar as the phonon dispersion relation of a lattice. Directly related to the pair potential, the dispersion factor is associated with the second and fourth derivatives of the pair potential at $r_{\rm vib}$. The divergent behavior given in Eq. (14) is exactly the same as that of the van Hove singularity in the phonon spectrum of a one-dimensional monatomic lattice chain.[31]

The successful prediction on the positions of the singularities in the INM spectrum by the picture of the isolated MNN pair indicates that the MNN pairs indeed play a dominant role on producing the singularities. However, the behavior of the binary-mode DOS given in Eq. (14) is quite different from the shape of the cusp shown in Fig. 2. What is missing in the picture of the isolated MNN pair is the interactions between each MNN pair and the rest particles in the fluid. If the range of the pair potential is extremely short, the interactions are generally much weaker than that within the two particles of a MNN pair, due to larger separations between anyone particle of the pair and the rest ones in the fluid. Because of the interactions, in each Hessian matrix, each 6×6 block which produces the binary modes of an isolated MNN pair is weakly coupled with other blocks in the matrix. Therefore, beyond the isolated-MNN-pair picture, we treat the blocks coupling the MNN pairs with the rest particles by the perturbation theory as given in Ref. 18, in which only the vibrational binary modes of those MNN pairs with separations less than the particle diameter are considered in order to interpret the INM spectrum in the high-frequency end of the real branch. But, our situation is somewhat different: Since the cusp is located in the intermediate region of the INM spectrum, both rotational and vibrational binary modes with frequencies near the position of the cusp have to be considered. Justified by numerical examinations for the LJ $2n$-n fluid of $n=18$ at $\rho^*=0.3$, the resonant effects between any two binary modes which are almost the same in frequency but belong to two different MNN pairs can be neglected, and this much simplifies the perturbation theory. Up to the first order, the perturbed vibrational binary frequency $\omega_{\rm vib}(i,j)$ of a MNN pair with particle index i and j is determined by the formula,

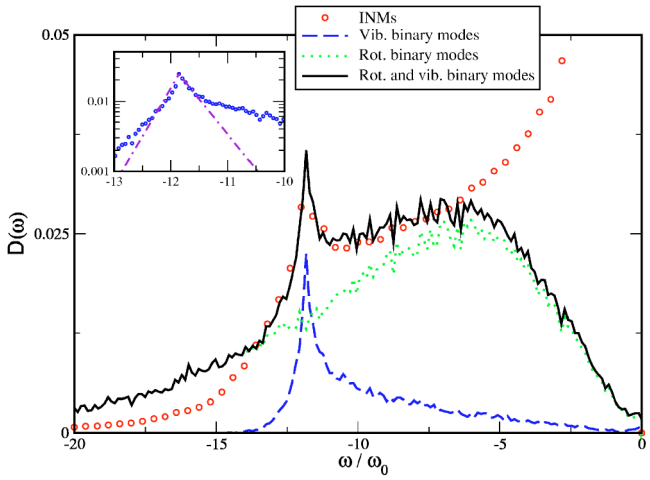

FIG. 6. Comparison between the DOS of the INMs and the binary-mode DOS of the perturbed MNN pairs in the LJ $2n$-n fluid for $n=18$ at $\rho^*=0.3$ and $T^*=1.4$. The open circles are for the DOS of the INMs. The dotted and dashed lines are for the DOS of the perturbed rotational and vibrational binary modes, respectively, and the solid line is their sum. The numerical curve of the INMs was obtained from an average of 100 configurations taken from MD simulations of 864 particles, and those of the perturbed binary modes were an average of 1000 configurations also for 864 particles. In the inset, the DOS of the perturbed vibrational binary modes (the symbols) is displayed in a logarithmic scale. On each side of the cusp, the data of the DOS is fitted by a linear line.

$$\omega^2_{\rm vib}(i,j) = \omega^2_{\rm vib,0}(r_{ij}) + \Delta\omega^2_{\rm vib}(i,j), \tag{16}$$

with

$$\Delta\omega^2_{\rm vib}(i,j) = \frac{1}{2} \sum_{l\neq i,j} \hat{\mathbf{r}}_{ij} \cdot [\mathbf{t}(\mathbf{r}_{il}) + \mathbf{t}(\mathbf{r}_{jl})] \cdot \hat{\mathbf{r}}_{ij}, \tag{17}$$

where l is the index for the rest particles and $\mathbf{r}_{il}$ is the positional vector from particle l to particle i. On the other hand, due to the double degeneracy of the rotational binary modes of a MNN pair in the zeroth order, the perturbed rotational binary frequency $\omega_{\rm rot}(i,j)$ is calculated by the degenerate perturbation theory and is given by

$$\omega^2_{\rm rot}(i,j) = \omega^2_{\rm rot,0}(r_{ij}) + \lambda_{\rm rot}(i,j) \tag{18}$$

with $\lambda_{\rm rot}(i,j)$ to be anyone of the eigenvalues of a two-dimensional square matrix with elements

$$S_{\alpha\beta}(i,j) = \frac{1}{2} \sum_{l\neq i,j} \hat{\theta}_\alpha(i,j) \cdot [\mathbf{t}(\mathbf{r}_{il}) + \mathbf{t}(\mathbf{r}_{jl})] \hat{\theta}_\beta(i,j), \tag{19}$$

where both α and β can be either 1 or 2. $\hat{\theta}_1(i,j)$ and $\hat{\theta}_2(i,j)$ are the three-dimensional eigenvectors of the two degenerate rotational binary modes in the zeroth order. Due to the perturbation, the two perturbed rotational binary frequencies of a MNN pair are no longer degenerate.

The binary-mode DOS of the perturbed MNN pairs, $D_\eta(\omega)$, is defined similarly as that of the isolated MNN pairs, just be replacing the frequency $\omega_{\eta,0}(r_{ij})$ in Eq. (8) with the perturbed binary-mode frequency $\omega_{\rm vib}(i,j)$ or $\omega_{\rm rot}(i,j)$ given in Eq. (16) or (18), respectively. For the LJ $2n$-n fluid of $n=18$ at $\rho^*=0.3$ and $T^*=1.4$, the results of the calculated $D_{\rm vib}(\omega)$ and $D_{\rm rot}(\omega)$ are shown in Fig. 6, in which their sum is compared with the imaginary-INM spectrum.[32] In the re-

sults of the first-order correction, $D_{\mathrm{vib}}(\omega)$ crosses over the sharp boundary at $|\omega^*_{\mathrm{vib},0}|$ of the vibrational-binary-modes DOS in the zeroth order, and decays fast beyond $|\omega^*_{\mathrm{vib},0}|$. Under our numerical accuracy, the divergence at the boundary of the DOS in the zeroth order is smeared out due to the perturbation and replaced by a cusp with a finite value.[33] Near the cusp, as shown in the inset of Fig. 6, $D_{\mathrm{vib}}(\omega)$ on each side of the cusp can be fitted by an exponential function decaying from the cusp; the decay rate on the high-frequency side is slightly larger. On the other hand, the MNN pairs whose rotational binary-mode frequencies are imaginary have pair separations in the repulsive part of the pair potential. Therefore, no singularity in the imaginary branch is resulted from the rotational binary modes; even under the perturbation, $D_{\mathrm{rot}}(\omega)$ is expected to be smooth for all imaginary frequencies. As shown in Fig. 6, the sum of $D_{\mathrm{vib}}(\omega)$ and $D_{\mathrm{rot}}(\omega)$ generally catches the behavior of the INM spectrum around the cusp: A good agreement between the two spectra is found in a region roughly from $7\omega_0$ to $13\omega_0$ in the imaginary-frequency branch, except for the imaginary frequencies with absolute values slightly less than $|\omega^*_{\mathrm{vib},0}|$. These good results given by the theory of the first-order perturbation are attributed to the short-range nature of the pair potential and low density of the fluid, which make the MNN pairs producing the cusp only experience a weak perturbation from their nearby neighbors. Physically, these results clearly indicate that the cusp in the INM spectrum is caused by the perturbed vibrational binary modes of those MNN pairs with separations close to the distance corresponding to the minimum vibrational curvature of the pair potential. Thus, we suggest that the singular behavior in the INM spectrum of the LJ $2n$-n fluids can be considered as a counterpart of the van Hove singularities in the phonon spectrum of a lattice.

IV. CONCLUSIONS

In this paper, we have studied the INM spectra of the LJ $2n$-n supercritical fluids for several values of n and fluid densities, in order to investigate the possibility for the existence of singularities in the vibrational spectra of topologically disordered systems, which do not possess a lattice reference frame. We study the LJ $2n$-n fluids for two reasons: First, the attractive range of the pair potential can be tuned by only one parameter n. Second, for each n, the vibrational curvature of the pair potential, which is the second derivative of the potential, has one minimum, and the rotational curvature, which is the first derivative of the potential divided by the radial distance, has one maximum. Both positions of the minimum and the maximum are in the attractive part of the pair potential. Also, the values of the minimum vibrational curvature and the maximum rotational curvature are soly determined by the parameter n.

At low-enough fluid densities, we have found the appearance of singularities in the INM spectra of the LJ $2n$-n fluids; a singularity may be a shoulder or a cusp depending on the value of n and the fluid density. For example, for $n=18$, which we study most, a singularity starts to appear as a shoulder in the imaginary spectrum at intermediate fluid densities. At low densities, the singularity in the imaginary branch changes to be a cusp, and at the same time a shoulder appears in the real branch. The singularity found in the imaginary branch is dominated by the vibrational binary modes of the MNN pairs with their pair separations corresponding to the minimum vibrational curvature of the pair potential, and that in the real branch is conceivably associated with the rotational binary modes of the MNN pairs with pair separations corresponding to the maximum rotational curvature. Generally, there are two ways to increase the amounts of those MNN pairs in a fluid, which is a key factor to decide whether a singularity exists or not: either by reducing the density of the fluid or by reducing the attractive range of the pair potential, which makes the extrema of the potential curvatures shift toward the center of the pair potential. On the other hand, these MNN pairs experience a perturbation from the rest particles in the fluid, and the perturbation tends to smear out the singularity. Increasing with the fluid density, the strength of the perturbation strongly influences the shape of a singularity. This interprets why a singularity changes from a cusp to a shoulder by increasing the fluid density.

The singularities in the INM spectrum of a simple fluid can be viewed as a counterpart of the van Hove singularities in the phonon spectrum of a lattice. The vibrational and rotational curvatures of the pair potential, whose extrema decide the positions of the singularities in the INM spectrum, act in some sense as the phonon dispersion relation of a lattice. Without the perturbation from the background of the fluid, the binary-mode DOS of the MNN pairs diverges at the singularity position, with its divergent behavior exactly the same as that of the van Hove singularity in the phonon spectrum of a one-dimensional momatomic lattice chain. However, the characters of the INMs to produce the singularities are quite different from those normal modes to produce the boson peak in the lattice models of disordered force constants. Based on the binary-mode picture, the INMs to produce the singularities are localized in nature, and this localization cannot be predicted by the mean-field theory. Also, those INMs in the imaginary branch are considered to be longitudinal in character and those in the real branch to be transverse.

Generally speaking, the lower the density of a simple fluid whose pair potential has an attractive part, the higher the possibility for the appearance of the singularities in the INM spectrum of the fluid. The general tendency shifts toward higher density as the attractive range of the pair potential is reduced. Realistically, for glasses and supercooled liquids with extremely short-range attractions, the cooperation of the binary rotations or librations at the extreme frequencies has a chance to bring about a resonant peak in the vibrational spectrum, in case that the number of these binary pairs is large enough. This conjecture is consistent with a recent interpretation for the origin of the boson peak in vitreous silica.[34]

ACKNOWLEDGMENT

T.-M.W. acknowledges support from the National Science Council of Taiwan under Grant No. NSC 93-2112-M009026.

[1]W. Schirmacher, G. Diezemann, and C. Ganter, Phys. Rev. Lett. **81**, 136 (1998).
[2]S. N. Taraskin, Y. L. Loh, G. Natarajan, and S. R. Elliott, Phys. Rev. Lett. **86**, 1255 (2001).
[3]S. N. Taraskin and S. R. Elliott, J. Phys.: Condens. Matter **14**, 3143 (2002).
[4]J. W. Kantelhardt, S. Russ, and A. Bunde, Phys. Rev. B **63**, 064302 (2001).
[5]*Amorphous Solids. Low Temperature Properties*, edited by W. A. Philips (Springer, Berlin, 1981).
[6]A. P. Sokolov, U. Buchenau, W. Steffen, B. Frick, and A. Wischnewski, Phys. Rev. B **52**, R9815 (1995).
[7]S. R. Elliott, *Physics of Amorphous Materials*, 2nd ed. (Longmans, New York, 1990).
[8]L. van Hove, Phys. Rev. **89**, 1189 (1953).
[9]R. M. Stratt, Acc. Chem. Res. **28**, 201 (1995).
[10]T. Keyes, J. Phys. Chem. A **101**, 2921 (1997).
[11]T. M. Wu and R. F. Loring, J. Chem. Phys. **97**, 8568 (1992).
[12]Y. Wan and R. M. Stratt, J. Chem. Phys. **100**, 5123 (1994).
[13]M. Mèzard, G. Parisi, and A. Zee, Nucl. Phys. B **559**, 689 (1999).
[14]V. Martin-Mayor, M. Mèzard, G. Parisi, and P. Verrocchio, J. Chem. Phys. **114**, 8068 (2001).
[15]T. S. Grigera, V. Martin-Mayor, G. Parisi, and P. Verrocchio, Phys. Rev. Lett. **87**, 085502 (2001).
[16]S. Ciliberti, T. S. Grigera, V. Martin-Mayor, G. Parisi, and P. Verrocchio, J. Chem. Phys. **119**, 8577 (2003).
[17]S. N. Taraskin and S. R. Elliott, Phys. Rev. B **65**, 052201 (2002).
[18]R. E. Larsen, E. F. David, G. Goodyear, and R. M. Stratt, J. Chem. Phys. **107**, 524 (1997).
[19]W. C. K. Poon, J. Phys.: Condens. Matter **14**, R859 (2002), and references therein.
[20]M. Hasegawa and K. Ohno, J. Phys.: Condens. Matter **9**, 3361 (1997).
[21]M. Hasegawa, J. Chem. Phys. **108**, 208 (1998).
[22]T. M. Wu and S. L. Chang, Phys. Rev. E **59**, 2993 (1999).
[23]G. A. Vliegenthart, J. F. M. Lodge, and H. N. W. Lekkerkerker, Physica A **263**, 378 (1999).
[24]T. M. Wu, W. J. Ma, and S. F. Tsay, Physica A **254**, 257 (1998).
[25]R. E. Larsen and R. M. Stratt, Chem. Phys. Lett. **297**, 211 (1998).
[26]R. E. Larsen and R. M. Stratt, J. Chem. Phys. **110**, 1036 (1999).
[27]J. Jang and R. M. Stratt, J. Chem. Phys. **113**, 5901 (2000).
[28]A. Medina, J. M. M. Roco, A. Calvo Hernandez, and S. Velasco, J. Chem. Phys. **119**, 5176 (2003).
[29]In Ref. 18, the binary mode of a MNN pair is only referred for the vibrational motion of the two particles.
[30]In principle, $\hat{\theta}_1(i,j)$ and $\hat{\theta}_2(i,j)$ can be any two mutually orthogonal unit vectors in the plane normal to $\hat{\mathbf{r}}_{ij}$. In this paper, we choose $\hat{\mathbf{r}}_{ij}, \hat{\theta}_1(i,j)$, and $\hat{\theta}_2(i,j)$ to be a set of spherical polar coordinates $(\hat{\mathbf{r}}, \hat{\theta}, \hat{\varphi})$, with $\hat{\mathbf{r}}$ equal to $\hat{\mathbf{r}}_{ij}$, relative to the reference frame of the simulation cubic box.
[31]N. W. Ashcroft and N. D. Mermin, *Solid State Physics* (Harcourt Brace College, New York, 1976).
[32]To investigate any finite-size effects of the MD simulation on the numerical data of the perturbed binary-mode DOS shown in Fig. 6, we have performed similar calculations for 500 configurations of 1728 particles and 2000 configurations of 432 particles at the same thermodynamic conditions. The results turn out to be that there is no noticeable difference around the cusp in the curves obtained from 1728 and 864 particles. For the system of 432 particles, the system size has some weak effect on the width of the cusp, which is slightly narrower than those of 864 and 1728 particles. This investigation indicates that the system size of 864 particles is large enough to neglect the boundary effects of the MD simulation box on the perturbation calculations for the numerical curves shown in Fig. 6.
[33]We have tested the numerical accuracy of our calculations for the cusp in the DOS of the perturbed vibrational binary modes by dividing the width of the frequency histograms into half. The results show that the shape of the cusp does not change at all.
[34]E. Duval, A. Mermet, R. Le Parc, and B. Champagnon, Philos. Mag. **84**, 1433 (2004).